engineering proceedings

MDPI

Proceeding Paper

Architecture of a Piezoelectric Acoustic Detector for Applications in Tissue and Soft Material †

Raúl Alberto Reyes-Villagrana [1,2]

[1] SECIHTI, Av. Insurgentes Sur 1582, Col. Crédito Constructor, Alcaldía Benito Juárez, Mexico City 03940, Mexico; rareyesvi@secihti.mx or rreyes@uaz.edu.mx
[2] Unidad Académica de Ciencia y Tecnología de la Luz y la Materia, Universidad Autónoma de Zacatecas, Zacatecas City 98160, Mexico

† Presented at the 12th International Electronic Conference on Sensors and Applications (ECSA-12), 12–14 November 2025; Available online: https://sciforum.net/event/ECSA-12

Abstract

There are various non-destructive techniques for determining the internal properties of materials in fluids, semi-solids, solids, and biological tissue. One of these techniques is low intensity ultrasonic testing. In this proceeding, a study on the architecture of a piezoelectric acoustic detector (PAD) is presented, from which the analysis for design, development and construction of the acoustic wave detector in the ultrasonic spectrum has emerged. Its aim is to apply it to soft matter and tissue. The 110 μm thick polyvinylidene fluoride (PVDF) piezoelectric element was used as the active element in the thickness mode configuration. Piezoelectric constitutive equations were applied to a one-dimensional model for the analysis. A cylindrical iron-nickel backing was used, and the parts were bonded with silver conductive epoxy glue. The results are presented. The equation for the output voltage of the piezoelectric acoustic detector is described. Functional testing of the PAD is demonstrated using the pulse-echo technique, in which an acoustic wave generator excited an ultrasonic immersion sensor in emission configuration and the DAP was connected to a digital oscilloscope to observe the received signal. Finally, pulsed photoacoustic spectroscopy was applied to a biological tissue emulator and yielded significant results in detection of a ruby sphere embedded in the emulator. It is proposed to further investigation the DAP models in multilayer structural configurations to increase their sensitivity.

Keywords: acoustic detector; model; piezoelectric; PVDF; ultrasound

Academic Editor(s): Name

Published: date

Citation: Reyes-Villagrana, R.A. Architecture of a Piezoelectric Acoustic Detector for Applications in Tissue and Soft Material. *Eng. Proc.* **2025**, *5*, x. https://doi.org/10.3390/xxxxx

1. Introduction

The development of new devices to monitor a particular process or, where appropriate, to modify a measuring element is carried out in the field known as electronic instrumentation. In this context, one of the branches of instrumentation is metrology, whose main objective is to obtain information about a physical process and find a suitable way to present this information to the observer or another technical system [1].

A sensor is a device that converts a physical phenomenon into an electrical signal. As such, sensors represent the part of the interface between the physical world and the world of electronic devices [2].

2. Modeling of Piezoelectric Acoustic Detector

The piezoelectric element is considered as an active material for the design of a piezoelectric acoustic detector (PAD) in thickness mode. For analysis purposes, it is necessary to consider the active element, the connecting cable and the signal conditioning as a single overall system. The impedance of piezoelectric material is generally very high. Therefore, the input impedance of the signal conditioning is almost always high impedance and is used for buffering rather than voltage amplification [3]. The cable capacitance can be considerable, especially with long cables. If a constant (quasi-static) pressure is applied to a single piezoelectric and maintained, a voltage is generated at the connection of the piezoelectric, but this is dissipated by the leakage resistance of the piezoelectric, R_S. Since this resistance, R_S, is very large (in the order of $10^{11}\Omega$) [4], this decrease would be very slow and perhaps allow at least a quasi-static response. However, if an instrument to measure the external voltage is connected to the piezoelectric, the charge will drop very quickly and prevent the measurement of the static stress. Therefore, consider Figure #, which shows a diagram containing within a rectangular figure a piezoelectric element, connected by a cable to the signal conditioning stage (which may include a filter and signal amplification stage) and which is referred to as the sensor, and this las part is connected to the controller.

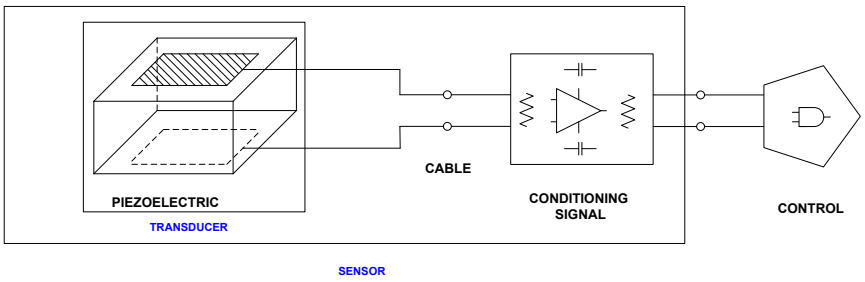

Figure 1. Block diagram of the piezoelectric element, the cable, and the signal processing.

Now consider a charge Q generated by a piezoelectric element, which can be expressed as follows,

$$Q = \Gamma_{33} \cdot P_P \tag{1}$$

where, Q is the charge, $\Gamma_{33} = g_{33} \cdot \gamma \cdot C_0$, g_{33} is the stress constant in the thickness mode, the thickness of the piezoelectric material, and C_0 is the capacitance between the electrodes; Pp is the average pressure exerted in the perpendicular direction on the surface of the piezoelectric material.

To simplify the system, an electrical circuit diagram corresponding to Figure 2 is obtained,

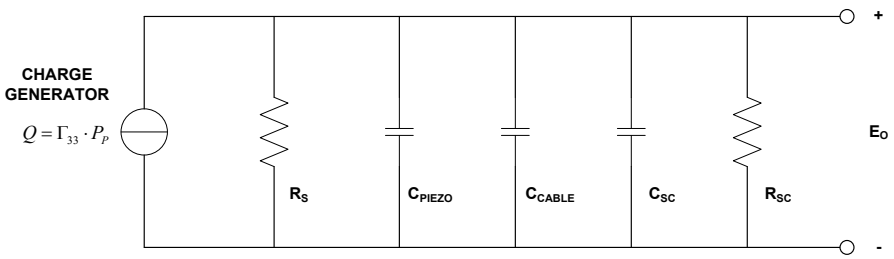

Figure 2. Schematic representation of the system.

Where R_S is the leakage resistance of the piezoelectric element C_{PIEZO} is the capacitance of the piezoelectric C_{CABLE} is the cable capacitance, C_{SA} and R_{SA} are the input capacitance and the resistance of the signal conditioning, respectively. All elements in parallel configuration.

Figure 3 is simplified by connecting a resistor and a capacitor in parallel and converting the charge generator into a current generator, i.e.,

$$I_{PIEZO} = \frac{dQ}{dt} = \Gamma_{33}\left(\frac{dP_P}{dt}\right) \tag{2}$$

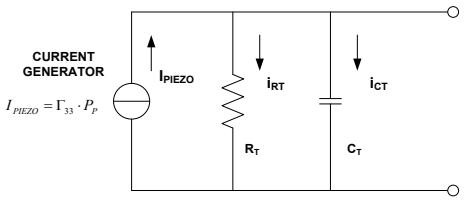

Figure 3. Simplified schematic representation.

Where R_T is the total resistance resulting from the parallel connection of R_{SA}; we disregard R_S for the reasons mentioned above; C_T is the total parallel capacitance of C_{PIEZO}, C_{CABLE}, and C_{SA}, i.e.,

$$R_T = R_{SA} \tag{3}$$

$$C_T = C_{PIEZO} + C_{CABLE} + C_{SA} \tag{4}$$

The simplification of the schematic diagram in Figure 4 is shown,

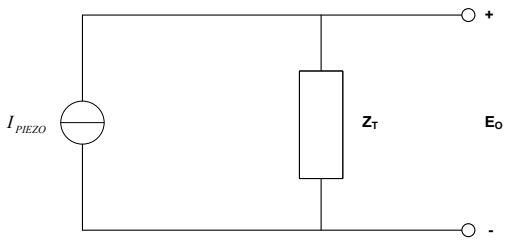

Figure 4. Simplified general representation.

Where Z_T is the parallel between C_T and R_T, i.e., $Z_T = C_T \,||\, R_T$.

Taking the Equation (2) and solving for $\tilde{E}_0(s)$ in the Laplace domain, it is described,

$$\tilde{E}_0(s) = \frac{s\eta\Gamma_S}{s\mu + 1} P_P \tag{5}$$

where, $\eta = C_T R_T$ and $\Gamma_S = \Gamma_{33} C_T$.

For the system architecture, Figure 5 was supplemented with the missing parameters as shown below,

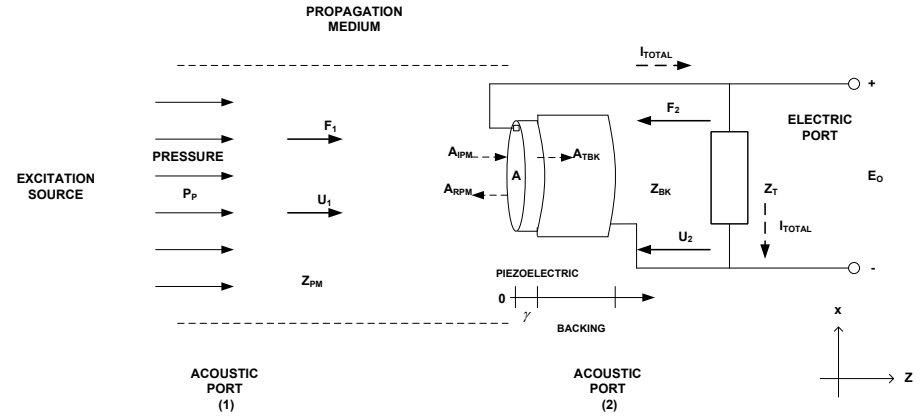

Figure 5. Sketch of the global system.

Figure 5 describes the piezoelectric active layer located between two semi-infinite isotropic media, labelled Z_{PM} and Z_{BK}, representing the acoustic impedance of the propagation medium and the backing, respectively. The width of the piezoelectric layer has the thickness γ.

P_P stands for the average pressure over the surface of the piezoelectric material. A_{IPM} is the amplitude of the incident wave; A_{RPM}, is the amplitude of the reflected acoustic wave and A_{TBK}, is the amplitude of the transmitted acoustic wave, F_1 and F_2 are the external mechanical forces on both sides. U_1 and U_2 are the velocities of the two surfaces, they are positive when they enter the detector from the left side). A is the surface area of the piezoelectric element face. Z_T is the total electrical impedance including the piezoelectric material, the cable and the signal conditioning E_0 is the output voltage (electrical stage) provided by the PAD. It is the total current through the electrical impedance.

By applying the piezoelectric constitutive equations and boundary conditions, we also analyze the internal structure of the piezoelectric acoustic detector elements and obtain the detector's output voltage expression.

$$\tilde{V}(s)=\frac{\dfrac{-h_{33}L_F\tilde{K}_F(s)E_0(s)}{sZ_P}}{1-\tilde{Z}_F(s)\left(\dfrac{K_F(s)L_F}{2}+\dfrac{K_B(s)L_B}{2}\right)\dfrac{k_t^2}{s}} \tag{6}$$

where Z_F is the transfer function of the influence of the external load with the secondary piezoelectric effect $\tilde{Z}_F(s)=\dfrac{1}{1+sC_0\tilde{Z}_T(s)}$ and Z_{EM} is the electromechanical impedance of the given PAD by $Z_{EM}(s)=\dfrac{1}{sC_0}\left\{1-\dfrac{k_t^2}{s}\left(\dfrac{K_F(s)L_F}{s}+\dfrac{K_B(s)L_B}{2}\right)\right\}$ [5,6].

In addition, $R_F=\dfrac{Z_P-Z_{PM}}{Z_P+Z_{PM}}$, $L_F=\dfrac{2Z_P}{Z_P+Z_{PM}}$, $R_B=\dfrac{Z_P-Z_{BK}}{Z_P+Z_{BK}}$, $L_B=\dfrac{2Z_P}{Z_P+Z_{BK}}$, $\tilde{K}_F(s)=\dfrac{\left(1-e^{-s\xi}\right)\left(1-e^{-s\xi}R_B\right)}{1-e^{-2s\xi}R_FR_B}$, and $\tilde{K}_B(s)=\dfrac{\left(1-e^{-s\xi}\right)\left(1-e^{-s\xi}R_F\right)}{1-e^{-2s\xi}R_FR_B}$.

3. Experimental Demonstration

Before the experimental test phase begins, a description of the design and construction of the piezoelectric acoustic detector is now presented.

3.1. Design and Construction of the Acoustic Detector with Monolayer Strcuture

The acoustic detector was designed with a monolayer structure, as shown in Figure 6.

(**a**) (**b**)

Figure 6. Design of the piezoelectric acoustic detector, (**a**) model; (**b**) real PAD.

The design consists of a (1) BNC electrical connector electrically connected to the (2) backing of iron-nickel alloy substrate using (3) conductive silver epoxy adhesive. The adhesive was also used to connect the carrier to backing side of the foil made of (4) piezoelectric PVDF material with a thickness of 110 μm and a diameter of 8.1 ± 1 mm; (5) a Kynar type conductor wire with a caliber of 30 AWG was used to electrically connect the other side of the piezoelectric material to the BNC connector. Finally, (6) the electrode of the backing body and the active layer were coated with an insulating epoxy adhesive and a heat insulating cover [7]. The PAD was then built, following the steps described above.

4. Results

Theoretically, the output voltage behavior of a monolayer system has the form shown in Figure 7. The input signal is a rectangular pulse with an amplitude P_P at a time T. the output signal E_0 has an exponential decay, and this behavior has to do with the intrinsic properties of the piezoelectric material.

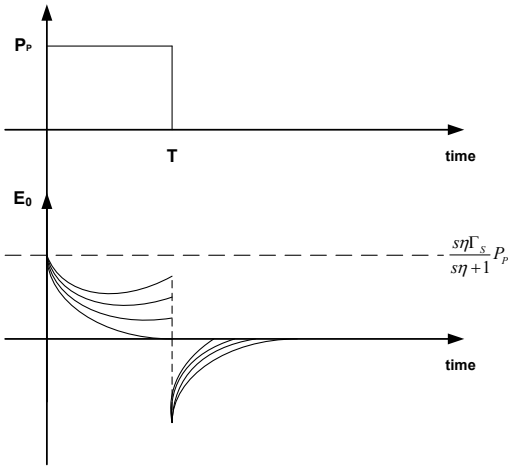

Figure 7. Modeling of the stimulus generated by a pulse on a piezoelectric monolayer leading to a voltage output.

A model for the excitation voltage by an input pulse was proposed via the PAD, as shown in Figure 8.

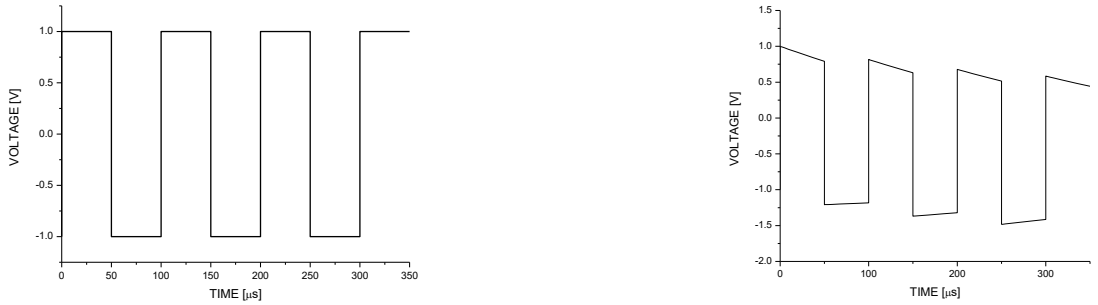

(**a**) (**b**)

Figure 8. (**a**) Stimulation by pulse-train voltage; (**b**) DAP output signal.

The experimental setup shown in Figure 9 was implemented with a function generator connected to an ultrasonic sensor (Parametrics V309) in the emitter setup and to channel 4 of the oscilloscope to observe the pulse train. The PAD was connected to channel 1 of the oscilloscope to observe the stimulation response generated by the emitter. Both the PAD and the sensor were placed parallel to each other in a glass vessel immersed in distilled water, which served as an acoustic propagation field (pulse-echo setup). The base on which the glass vessel stands is made of wood. The stimulation by the function generators was $1V_{P\text{-}P}$.

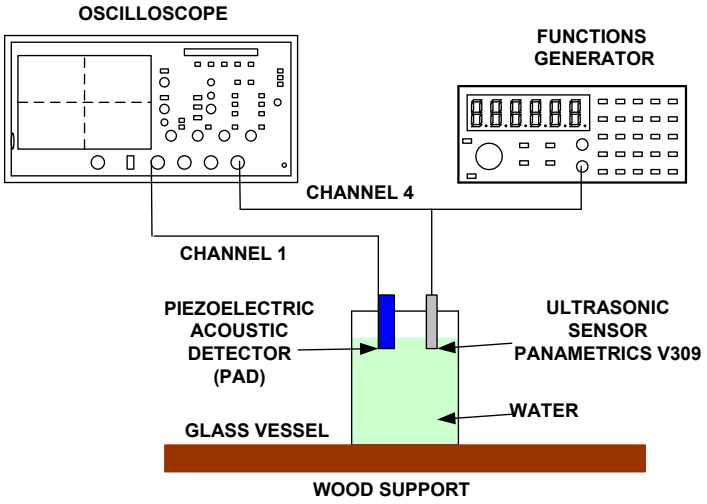

Figure 9. Experimental setup.

The output voltage in Figure 10a shows the same behavior as in Figure 10b the peaks and valleys of the pulse trains have smooth exponential decay, but exhibit a few disturbances, such as noise.

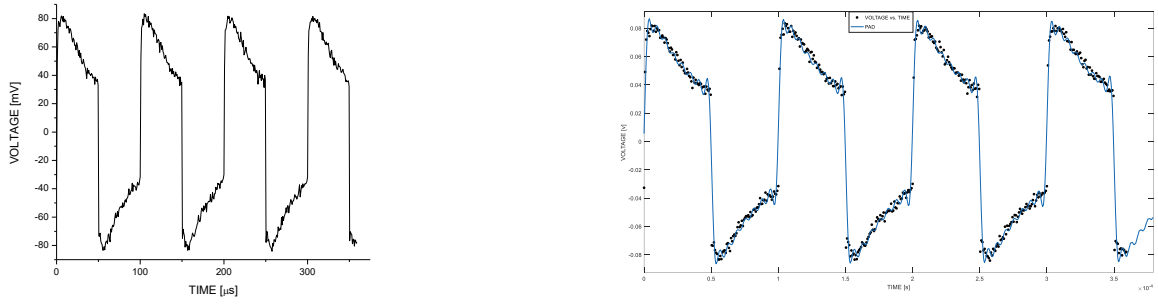

(**a**) (**b**)

Figure 10. (**a**) DAP output voltage; (**b**) Comparison between the model and the experimental stage.

To perform the experiment to detect the location and size of an object absorber (ruby sphere) with a diameter of 2.38 ± 0.001 mm, immersed in a phantom with the optical properties of a mammary gland as a means of propagation, the assembly was performed using the technique of spectroscopy pulsed photoacoustic. The signal is obtained through transmission mode setup, as shown in Figure 11.

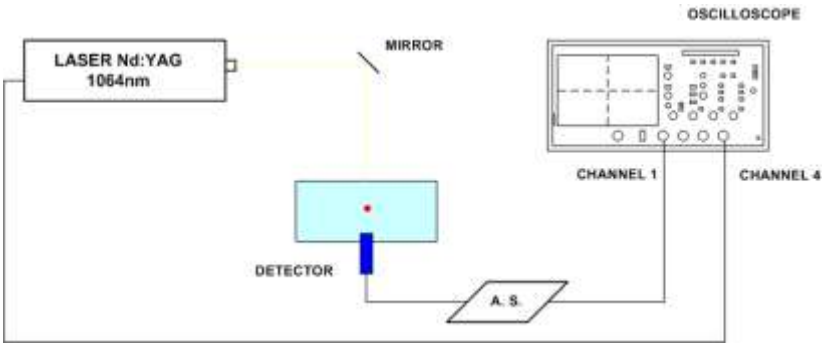

Figure 11. Experiment setup.

Used a Nd: YAG λ = 1064 nm, working with a frequency of 10 Hz and emitting a pulse a width of 9 ns, with a gaussian temporal profile and energy on the field 20 mJ ruby sphere. The laser shot was recorded by the oscilloscope channel 1. The ruby sphere was placed at a depth of 1.8 cm from the surface. The detector is mounted on the bottom of the container in the propagation medium and connected to a block of signal conditioning and then the signal was recorded by channel 4 of the oscilloscope. Figure 12 shows the signal obtained.

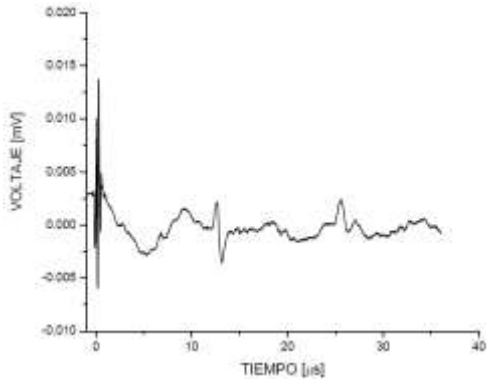

Figure 12. Photoacoustic signal obtained.

Figure 12 shows a first pulse for the laser beam shot, then describes the signal corresponding to the absorbing object detection in a time of 12.58 µs. The pulse width is about 2 µs. Finally, the observed signal in a time of 25.51 µs, corresponds to the echo signal absorbing a bandpass filter from 1 to 10 MHz.

It is necessary to comment on the following, which describes some conditions for the creation of the architecture of a PAD.

1. Determine beforehand the propagation medium in which the detector will operate to anticipate the losses that will occur.
2. Detector area A small offers better resolution. On the contrary, sensitivity decreases. However, this can be compensated by the signal conditions.
3. Most commercial detectors use piezoceramics due to their properties. The justification for using PVDF is that its acoustic impedance is closer to that of water and consequently like that of biological tissue. But it is also known that acoustic coupling, the detectors and the medium are under investigation.
4. It is necessary to use signal conditioning in the detectors, to homogenize the amplitude of the detector, i.e., to use filters when receiving the signal, then amplify it and finally filter again. It is also important to use devices with high switching power and minimal noise emission.

5. There is interest in extending the study to implement a piezoelectric acoustic detector with a multilayer internal structure to increase the output voltage generated by the piezoelectric material.

5. Conclusions

This proceeding described the study and development of a piezoelectric acoustic detector (PAD) for use used in soft matter.

The study involved the determination of an electrical equivalent system taking into account the propagation medium, the acoustic detector (external and internal parameters) and the peripheral connections.

The piezoelectric constitutive equations were used to obtain modeling to determine the general equation were used to develop a model that determined the general equation for the acoustic detector's output voltage.

An acoustic detector was constructed using the piezopolymer PVDF, as its acoustic impedance is like that of water, and, consequently, to that of biological tissue. A pulse-echo ultrasonic experiment was performed with an acoustic field provided by water to understand its basic operation.

An acoustic field experiment was also conducted using a phantom with the optical properties of the mammary gland and a ruby sphere embedded within the phantom. Pulse photoacoustic spectroscopy was applied to detect the position (depth) and size of the ruby sphere.

There is interest in continuing the study to implement a system with a multilayer structure, as well as the restructuring of its internal elements and experimental tests that include the signal to noise ratio (SNR).

Funding: This research received no external funding.

Institutional Review Board Statement: Not applicable.

Informed Consent Statement: Not applicable.

Data Availability Statement: The data used to support the findings of this study can be made available by the corresponding author request.

Acknowledgments: R.A.R.-V. gratefully acknowledges the support of IxM-SECIHTI, and LUMAT-UAZ.

Conflicts of Interest:

References

1. Regtien, P.P. *Electronic Instrument*, 2nd ed.; VSSD Press: The Netherlands; 2005.
2. Wilson, J.S. *Sensor technology handbook*, 1st ed.; Elsevier: Amsterdam, The Netherlands, 2005.
3. Pallás Areny, R.; Webster, J. *Sensor and Signal Conditioning*, 1st ed.; Wiley & Sons: Hoboken, NJ, USA, 2001.
4. Measurements specialties, Inc. *Piezo Film Sensor Technical Manual*, Rev 02 apr 99.
5. Hayward, G.; MacLeod, C.J.; Durrani, T.S. A system model of the thickness mode piezoelectric transducer. *J. Acoust. Soc. Am.* **1984**, *76*, 369–382.
6. Bentley, J.P. *Sistemas de Medición, Principios y Aplicaciones*, 1st ed.; CECSA: Mexico; 2000.
7. Chen, Q.X.; Payne, P.A. Industrial applications of piezoelectric polymer transducers. *Meas. Sci. Technol.* **1995**, *6*, 249–267.